

## Theory of Interedge Superexchange in Zigzag Edge Magnetism

J. Jung,<sup>1,\*</sup> T. Pereg-Barnea,<sup>2</sup> and A. H. MacDonald<sup>1</sup>

<sup>1</sup>*Department of Physics, University of Texas at Austin, Austin, Texas 78712, USA*

<sup>2</sup>*Department of Physics, California Institute of Technology, Pasadena, California 91125, USA*

(Received 3 December 2008; published 5 June 2009)

A graphene nanoribbon with zigzag edges has a gapped magnetic ground state with an antiferromagnetic interedge superexchange interaction. We present a theory based on asymptotic properties of the Dirac-model ribbon wave function which predicts  $W^{-2}$  and  $W^{-1}$  ribbon-width dependencies for the superexchange interaction strength and the charge gap, respectively. We find that, unlike the case of conventional atomic-scale superexchange, opposite spin orientations on opposite edges of the ribbon are favored by both kinetic and interaction energies.

DOI: 10.1103/PhysRevLett.102.227205

PACS numbers: 75.30.Et, 73.20.-r, 73.22.-f, 75.75.+a

*Introduction.*—Motivated by the seminal theoretical work of Kobayashi, Fujita, Nakada, Wakabayashi, and collaborators [1–4], and by progress in graphene preparation [5], researchers have recently [6–16] reexamined the intriguing physics of edge magnetism in zigzag terminated graphene nanoribbons from a number of different points of view. The magnetic state is a consequence of the nearly flat subbands which occur at the Fermi level in a neutral zigzag ribbon, and of the orbital character of the wave functions associated with these bands. There is still no conclusive [17] experimental evidence that a 1D magnetic state occurs in ideal zigzag ribbons, but the theoretically predicted state seems likely given that quite different electronic structure theories [from crude Hubbard models to elaborate *ab initio* density-functional-theory calculations] yield consistent [13] predictions and that there are at present no other ideas on how the unusual flat bands could be accommodated in the many-electron state. Present ribbons are far from ideal, however, and the main obstacle to realizing this paradigmatic example of  $d^0$  magnetism [18,19] may lie in furthering recent progress [20–22] toward chemistry and defect control at the edge.

Mean-field-theory calculations predict that the ground state of a zigzag ribbon has unusually stiff parallel spin alignment along each edge [12] and antiferromagnetic [14] interedge superexchange interactions. In this Letter we present a mostly analytic theory of the ribbon-width  $W$  dependence of the important interedge superexchange interaction. Our theory relies on the properties of large  $W$  solutions of the continuum model approximation [6] for zigzag edges. We predict that interedge interactions can have a substantial influence on the properties of these unusual 1D magnets.

*Ribbon edge-state bands.*—The  $\pi$ -orbital tight-binding model for a finite width ribbon yields a number of 1D Bloch bands proportional to the ribbon width [15]. To a high degree of accuracy, zigzag magnetism is a rearrangement of only [13] the highest occupied ( $|k-\rangle$ ) and lowest unoccupied ( $|k+\rangle$ ) ribbon bands, whose transverse wave

functions are, respectively, odd and even functions of carbon atom sites across the ribbon. Since the exchange physics which favors magnetism is local, it is revealed most clearly by forming states in this Hilbert space which are localized as far as possible at one edge or the other,  $|kL/R\rangle = \frac{1}{\sqrt{2}}(|k-\rangle \pm |k+\rangle)$ , where we have chosen the band transverse wave function amplitudes to be positive at the leftmost atom. These left ( $L$ ) right ( $R$ ) basis states can be expanded in terms of amplitudes on atoms in the ribbon unit cell:  $|kL\rangle = L_{kl}|kl\rangle_B$ ,  $|kR\rangle = R_{kl}|kl\rangle_B$  with sums over sites  $l$  within the unit cell implied. It is readily verified that  $L_{kl}$  and  $R_{k'l'}$  are strictly localized on opposite sublattices so that  $L_{kl}R_{k'l'} = 0$ . In this representation, the  $\pi$ -band tight-binding model Hamiltonian  $H_{\text{TB}}(k) = t(k)\tau_x$  where  $\tau_x$  is a Pauli matrix and the left-right tunneling amplitude  $t(k) = -E_{\text{TB}}^-(k) = E_{\text{TB}}^+(k)$ . The bands in the Brillouin zone  $-\pi/a \leq k \leq \pi/a$  have periodicity  $2\pi/a$  and have inversion symmetry so we can restrict our attention to the interval  $0 \leq k \leq \pi/a$ . Zigzag edge magnetism follows from the following tight-binding model property [6,15]. For  $2\pi/3 + q_e a \leq |k|$ , where  $q_e = 1/W = 2/\sqrt{3}aN$ , the states  $|kL\rangle$  and  $|kR\rangle$  are exponentially localized near their respective edges and the left-right hopping amplitude  $t(k)$  decreases rapidly with increasing  $W$ . (Here  $a = 2.46 \text{ \AA}$  is the lattice constant and  $N$  is the number of atom pairs in the ribbon unit cell.) Over this region of wave vector  $|kL\rangle$  and  $|kR\rangle$  are proper edge states.

*Hubbard model mean-field theory.*—In order to explain our theory of the superexchange interaction we briefly summarize the mean-field theory of the magnetic state, which is particularly simple in the Hubbard model case. It is instructive to contrast two different collinear magnetic solutions of the mean-field equations, an antiferromagnetic (AFM) one in which spins have opposite orientations on opposite edges and a ferromagnetic (FM) one in which spins have the same orientation on opposite edges. The two  $LR$  basis spin-dependent mean-field Hamiltonians are given (up to a common constant) by

$$H_{\sigma}^{\text{AFM}} = \begin{pmatrix} -\sigma\Delta^{\text{AFM}} & t \\ t & \sigma\Delta^{\text{AFM}} \end{pmatrix}, \quad (1)$$

$$H_{\sigma}^{\text{FM}} = \begin{pmatrix} -\sigma\Delta^{\text{FM}} & t \\ t & -\sigma\Delta^{\text{FM}} \end{pmatrix},$$

where  $\sigma = +/ -$  for  $\uparrow / \downarrow$  spin, the  $k$  dependence of  $t$  and the self-consistent exchange potentials is implicit, and

$$\Delta^{\text{AFM}}(k) = U \sum_l L_{kl}^2 \langle m_l \rangle_{\text{AFM}}, \quad \Delta^{\text{FM}}(k) = U \sum_l L_{kl}^2 \langle m_l \rangle_{\text{FM}}. \quad (2)$$

In Eq. (2)  $m_l = (n_{\uparrow} - n_{\downarrow})/2$  is the site-dependent spin density and  $n_{l\sigma}$  is the spin-dependent mean occupation number at site  $l$ . [Both solutions have  $n_l \equiv (n_{\uparrow} + n_{\downarrow}) \equiv 1$ , a convenient property of neutral ribbons which can be traced to particle-hole symmetry in the paramagnetic bands.] These self-consistent solutions are illustrated for a  $N = 20$  zigzag ribbon in Fig. 1. Both the FM (even  $m_l$ ) and AFM (odd  $m_l$ ) state solutions are self-consistent. The mean-field equations are closed by evaluating  $m_l$  using

$$\langle m_l \rangle_{\text{AFM}} = \frac{a}{2\pi} \int_0^{\pi/a} dk (L_{kl}^2 - R_{kl}^2) P(k), \quad (3)$$

$$\langle m_l \rangle_{\text{FM}} = \frac{a}{2\pi} \int_{k_c}^{\pi/a} dk (R_{kl}^2 + L_{kl}^2), \quad (4)$$

where the degree of LR polarization is

$$P(k) \equiv \frac{\Delta^{\text{AFM}}(k)}{\{[\Delta^{\text{AFM}}(k)]^2 + t(k)^2\}^{1/2}} \quad (5)$$

In the AFM case, local spin polarization follows from the opposite left-right polarizations of  $\uparrow$  and  $\downarrow$  states whereas in the FM case the left-right polarization vanishes and spin polarization follows from double occupation of  $\uparrow$  bands for  $k_c < |k| < \pi/a$  where  $k_c$  is the wave vector at which the  $\uparrow$ ,  $+$  band and the  $\downarrow$ ,  $-$  band cross as illustrated in Fig. 1.  $\Delta^{\text{AFM}}$  and  $\Delta^{\text{FM}}$  are nearly (but not quite) identical because their  $m_l$ 's differ mostly in the middle of the ribbon which has little influence on the edge states.

*Ribbon-width scaling rules.*—From solutions of the graphene continuum model [6,15] we obtain for the region near  $k = \pm(2\pi/3 + q)$  and small  $q$  the expression

$$t[\pm(q + 2\pi/3)] = (\sqrt{3}\gamma_0 a/2) \sqrt{q^2 - z^2}, \quad (6)$$

where  $z$  satisfies, respectively, for  $q > q_e$  and  $q < q_e$ ,

$$zW \coth(zW) = qW, \quad zW / \tan(Wz) = qW. \quad (7)$$

In the continuum model we have for  $k_c < k < \pi/a$

$$R_{kl}^2 \rightarrow R_k^2(y) = 2z[\cosh(2zy) - 1]/[\sinh(2Wz) - 2Wz], \quad (8)$$

and for  $0 < k < k_c$

$$R_k^2(y) = 4z \sin(zy)/[2Wz - \sin(2Wz)]. \quad (9)$$

The left centered functions can be obtained through the symmetry relation  $L_{kl} = R_{k_{2N-l}}$ . It follows that

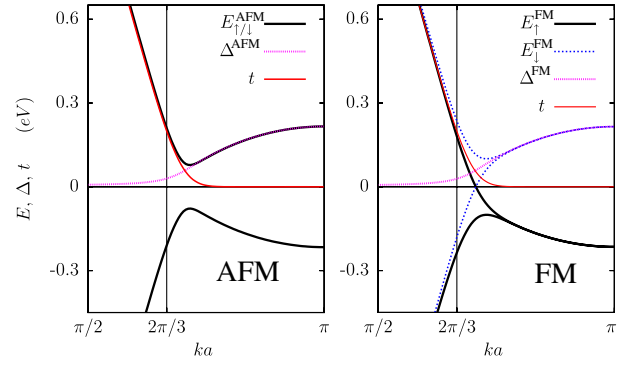


FIG. 1 (color online). Hubbard model mean-field calculations for  $\gamma_0 = 2.6$  eV and  $U = 2$  eV for a zigzag ribbon with  $N = 20$ . Left: Mean-field energy bands for the AFM state:  $E_{\uparrow/\downarrow}^{\text{AFM}}(k) = \pm[\Delta^{\text{AFM}}(k)^2 + t^2(k)]^{1/2}$  for both spins with the low-energy states of one spin concentrated on one side of the ribbon and the low-energy states of the opposite spin concentrated on the opposite side.  $t(k)$ , the left-right hopping parameter, is quite insignificant for this ribbon width in the edge-state region.  $\Delta^{\text{AFM}}(k)$  is dominant in the edge-state region because of large local spin polarizations. Right: Mean-field energy bands for the FM state:  $E_{\sigma}^{\text{FM}}(k) = \sigma\Delta^{\text{FM}}(k) \pm |t(k)|$ . Note that  $\Delta^{\text{AFM}}$  and  $\Delta^{\text{FM}}$  are nearly identical. The bands are periodic with periodicity  $2\pi/a$  and inversion symmetric.

$$t(k) = \frac{\gamma_0}{W} \tilde{t}(qW), \quad R_k(y)^2 = W^{-1} \chi^2(qW, y/W), \quad (10)$$

where the functions  $\chi^2(x)$  and  $\tilde{t}(x)$  are implicitly defined by the above equations. We have verified that these scaling relations apply accurately even in quite narrow ribbons.

From Eq. (2) we see that the Hubbard model exchange potentials depend on local spin polarizations  $\langle m_l \rangle$  which are large only close to the edge and approach a well-defined limit already for quite narrow ribbons; the form of the spin polarization near each edge is a single-edge property unrelated to interedge interactions. From this observation and the above scaling relations for the zigzag edge states, we propose the following scaling rule for the form of the exchange potential:

$$\Delta^{\text{AFM/FM}}(k) = W^{-1} \tilde{\Delta}^{\text{AFM/FM}}(qW). \quad (11)$$

Since both  $\tilde{\Delta}(k)$  and  $\tilde{t}(k)$  depend only on  $qW$ , it follows from Eq. (5) that  $P(k)$  also depends only on  $qW$ . We have verified numerically that this relationship holds accurately for sufficiently wide ribbons as illustrated in Fig. 2.

*Interedge interaction.*—The strength of the superexchange interaction which determines the alignment between magnetization directions on opposite edges is given by the total energy difference between AFM and FM solutions. Because the electrostatic Hartree energies of both states are identical, the energy difference per edge carbon atom  $\Delta E$  can be separated into band (kinetic) and exchange energy contributions; see Fig. 3:

$$\Delta E = E^{\text{FM}} - E^{\text{AFM}} = \Delta T + \Delta E_X. \quad (12)$$

The difference of kinetic energies between AFM and FM solutions is determined by

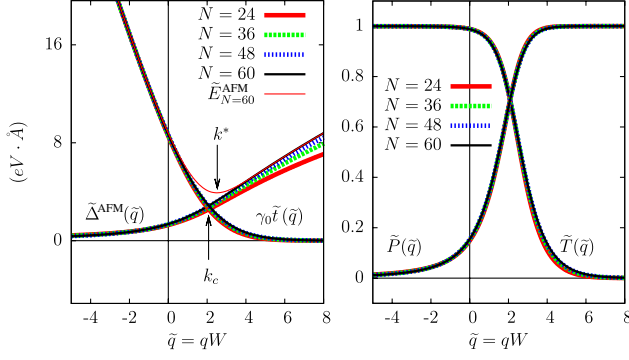


FIG. 2 (color online). Left: Dependence of  $\tilde{\Delta}^{\text{AFM}}$  and  $\gamma_0 \tilde{t}$  on the scaled coordinate  $\tilde{q} = qW$  and the corresponding  $N = 60$  AFM state quasiparticle bands. Note that the self-consistently calculated  $\tilde{\Delta}^{\text{AFM}}$  approaches a well-defined function at large  $N$ . The positions  $k_c$  and  $k^*$  are, respectively, the values of  $k$  at which  $\Delta^{\text{AFM}} = t$  and the band gap minimum occurs. Right: Scaling collapse of antiferromagnetic state self-consistent left-right polarization  $\tilde{P}$  and symmetric-antisymmetric polarization  $\tilde{T}$  represented in the scaled coordinate  $\tilde{q}$ . Note that  $P^2 + T^2 = 1$  by definition.

$$T^{\text{AFM}} = -\frac{2a}{\pi} \int_0^{\pi/a} dk t(k) T(k), \quad T^{\text{FM}} = -\frac{2a}{\pi} \int_0^{k_c} dk t(k), \quad (13)$$

where  $T(k) = [1 - P^2(k)]^{1/2}$  is the symmetric-antisymmetric polarization of AFM states. The FM as well as noninteracting band eigenstates have  $T(k) \equiv 1$ . In the noninteracting ground state the lower energy state is fully occupied and the total energy contains all the band energy. Both AFM and FM states sacrifice band energy contributions in the region  $|k| \geq 2\pi/3a$  in order to gain interaction energy. In the ferromagnetic case the band energy gain is sacrificed completely for  $|k| > k_c$ , the wave vector at which  $\Delta = t$ . At larger values of  $|k|$  both bonding and antibonding states are occupied for one spin and both are empty for the other spin. There is therefore an abrupt separation at  $|k| = k_c$  between wave vectors which contribute to band energy and regions which contribute to the exchange energy, discussed below. In the AFM case, on the other hand,  $T$  crosses smoothly as a function of scaled wave vector  $\tilde{q} = qW$  from the kinetic energy contributing regime at small  $|k|$  to the exchange energy contributing regime at large  $|k|$ . Using the scaling properties of  $t$  and  $\Delta$  the kinetic energy contribution to the difference can be written as an integral over  $\tilde{q}$ :

$$\Delta T = \frac{2a\gamma_0}{\pi W^2} \left\{ \int_{-\infty}^{\tilde{q}_c} d\tilde{q} \tilde{t}(\tilde{q}) [\tilde{T}(\tilde{q}) - 1] + \int_{\tilde{q}_c}^{\infty} d\tilde{q} \tilde{t}(\tilde{q}) \tilde{T}(\tilde{q}) \right\}. \quad (14)$$

The integrals in Eq. (14) converge at  $-\infty$  because  $\tilde{T}(\tilde{q})$  approaches 1 rapidly and at  $\infty$  because  $\tilde{T}(\tilde{q})$  approaches 0 rapidly. The contribution from  $\tilde{q} < \tilde{q}_c$  is negative while the contribution from  $\tilde{q} > \tilde{q}_c$  is positive. Substantial cancellation leads to a small kinetic energy contribution to  $\Delta E$ .

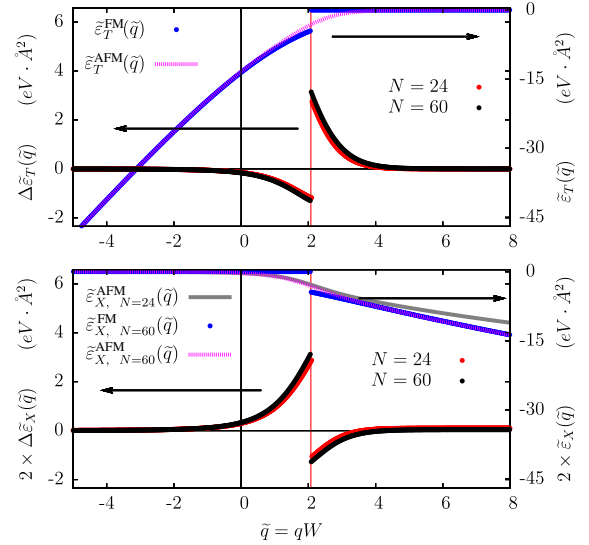


FIG. 3 (color online).  $k$ -resolved contributions to the kinetic ( $\tilde{\epsilon}_T$ ) (upper panel) and exchange (lower panel) energies ( $\tilde{\epsilon}_X$ ) of the FM and AFM states and the corresponding FM - AFM differences as a function of the scaled momentum coordinate  $\tilde{q} = qW$ .  $\tilde{\epsilon}_T^{\text{FM}}$  and  $\tilde{\epsilon}_T^{\text{AFM}}$  are the integrands in the kinetic energy expression Eq. (13), and  $\tilde{\epsilon}_X^{\text{FM/AFM}}$  is the corresponding quantity for the exchange interaction energy. The discontinuities in the ferromagnetic case are due to the crossing between the majority-spin symmetric and minority-spin antisymmetric bands at  $k_c$ , indicated by a thin vertical line. Although the kinetic energies roughly double the interaction energies at most  $k$  values, the exchange contribution to superexchange is much larger because of weaker cancellation between  $|k| < k_c$  and  $|k| > k_c$  regions.

The exchange energy integrands satisfy the scaling relations similar to the kinetic terms and we can write the exchange energy difference as

$$\Delta E_X = \frac{a}{\pi W^2} \left\{ \int_{-\infty}^{\tilde{q}_c} d\tilde{q} \tilde{\Delta}^{\text{AFM}}(\tilde{q}) \tilde{P}(\tilde{q}) + \int_{\tilde{q}_c}^{\infty} d\tilde{q} \tilde{\Delta}^{\text{AFM}}(\tilde{q}) \times [\tilde{P}(\tilde{q}) - 1] \right\} + \frac{1}{3} [\Delta^{\text{AFM}}(\pi/a) - \Delta^{\text{FM}}(\pi/a)]. \quad (15)$$

The first two terms are similar to the corresponding band energy contributions, with the discontinuity at  $q_c$  again due to the band crossing in the ferromagnetic state. We write this contribution to the superexchange interaction as  $J_X/W^2$ . An additional contribution appears because  $\Delta^{\text{AFM}}$  and  $\Delta^{\text{FM}}$  are not quite identical for  $\tilde{q} \rightarrow \infty$ .

In the Hubbard model we can relate the asymptotic difference in  $\Delta$  to the difference in spin polarization on the edge atom:  $\delta\Delta \equiv \Delta^{\text{AFM}}(\pi/a) - \Delta^{\text{FM}}(\pi/a) = U(\langle m_{\text{edge}} \rangle_{\text{AFM}} - \langle m_{\text{edge}} \rangle_{\text{FM}})$ . Labeling the leftmost site as site 1, noting that  $R_{k1}^2 = 0$ , and recalling the definitions of  $\langle m_l \rangle$  in Eqs. (3) and (4), we find that

$$\delta\Delta = \frac{a}{2\pi} \int_0^{k_c} dk L_{k1}^2 P(k) + \frac{a}{2\pi} \int_{k_c}^{\pi/a} dk L_{k1}^2 [1 - P(k)] \equiv \frac{3J_{\delta m}}{W^2}. \quad (16)$$

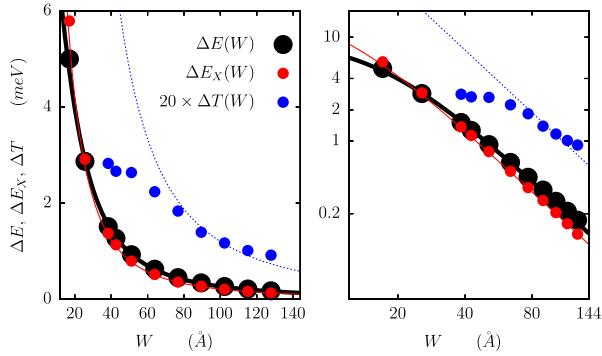


FIG. 4 (color online). The difference between the FM and AFM states in total energy ( $\Delta E$ ), exchange energy ( $\Delta E_X$ ), and kinetic energy ( $\Delta T$ ) plotted on a linear scale (left) and a logarithmic scale (right). The total energy difference follows a  $W^{-2}$  decay law at large  $W$  and is dominated by exchange energy contribution. The kinetic energy contribution is substantially smaller and the asymptotic decay law develops only for sufficiently large ribbon width. The total energy  $\Delta E$  was fitted with  $2.7/(W^2 + 280)$ , the exchange energy  $\Delta E_X$  with  $2.1/(W^2 + 100)$ , and the fitting for the kinetic contribution was obtained from the difference between both resulting in  $0.6/W^2$  (represented with  $\times 20$  magnification), all terms given in  $\text{eV} \text{ \AA}^{-2}$  units. 12 K  $k$  points were sampled in the 1D Brillouin zone.

Adding the three contributions we obtain

$$\Delta E(W) = W^{-2}(J_K + J_X + J_{\delta m}). \quad (17)$$

For  $\gamma_0 = 2.6 \text{ eV}$  and on site repulsion  $U = 2.0 \text{ eV}$  that results in band gaps similar to local-density approximation [13], we find that the kinetic and exchange contributions to the interaction are  $J_K = 0.6 \text{ eV} \cdot \text{ \AA}^2$ , and  $J_X + J_{\delta m} = 2.1 \text{ eV} \cdot \text{ \AA}^2$ . (See Fig. 4.) Separately  $J_{\delta m} \approx 1.15 \text{ eV} \cdot \text{ \AA}^2$  implying that the interaction contribution is composed in approximately equal measures of contributions from  $q$  near  $q_c$  and contributions far in the edge regime.

**Conclusions and discussions.**—Our analysis shows that the antiferromagnetic interedge superexchange interaction in magnetic zigzag nanoribbons is the sum of three contributions (band energy, exchange energy, and edge spin polarization), all of which arise from a region of the ribbons' 1D Brillouin zone which is centered on  $|k| = 2\pi/3a$  and scales in width as  $1/W$ . Unlike the familiar case of atomic-scale superexchange interactions, in which antiferromagnetic spin arrangements lower the kinetic energy at a cost in interaction energy, all three contributions have the same sign—with the kinetic contribution being substantially smaller in magnitude. Our conclusions rest primarily on analytic properties of continuum model solutions to the  $\pi$ -band model for zigzag nanoribbons and depend on the particle-hole symmetry of graphene's conduction and valence bands. We have demonstrated numeri-

cally that the continuum model predictions are accurate, even in narrow nanoribbons. Although some details of our analysis depend on the simplified Hubbard model we use, we expect the scaling properties of states near  $|k| = 2\pi/3a$  to be general and that our qualitative conclusions will apply to any mean-field-theory treatment of zigzag ribbon magnetism.

Collective spin behavior is expected [12] to be important in zigzag ribbon magnets, even though they are one dimensional, because of the exceptionally strong exchange interactions along each edge. Assuming that the magnetic anisotropy (which is expected to be weak) is important only at low temperatures, the correlation length  $\xi$  along an isolated zigzag edge is estimated [12] to be  $\sim 3000 \text{ \AA}/T$  [K]. Since the interedge interaction arises from an interval of  $k$  space with width  $1/W$ , its range along the edge will be  $\sim W$ . When  $\xi$  is smaller than  $W$ , interedge interactions will have little influence. For  $\xi$  larger than  $W$ , the interedge interactions will help suppress thermal magnetization fluctuations.

The authors gratefully acknowledge helpful interactions with R. Bistritzer, J. Hill, H.-H. Lin, N. Sinitsyn, J. Fernández-Rossier, J. J. Palacios, and C.-C. Wang. This work was supported by the Welch Foundation, NRI-SWAN, ARO, DOE, and by the Spanish Ministry of Education through the MEC-Fulbright program.

\*jeil@physics.utexas.edu

- [1] K. Kobayashi, Phys. Rev. B **48**, 1757 (1993).
- [2] M. Fujita *et al.*, J. Phys. Soc. Jpn. **65**, 1920 (1996).
- [3] K. Nakada *et al.*, Phys. Rev. B **54**, 17954 (1996).
- [4] K. Wakabayashi *et al.*, Phys. Rev. B **59**, 8271 (1999).
- [5] K. S. Novoselov *et al.*, Nature (London) **438**, 197 (2005).
- [6] L. Brey and H. A. Fertig, Phys. Rev. B **73**, 235411 (2006).
- [7] K.-I. Sasaki *et al.*, J. Phys. Soc. Jpn. **75**, 074713 (2006).
- [8] T. Hikihara *et al.*, Phys. Rev. B **68**, 035432 (2003).
- [9] Y.-W. Son *et al.*, Phys. Rev. Lett. **97**, 216803 (2006).
- [10] Y.-W. Son *et al.*, Nature (London) **444**, 347 (2006).
- [11] L. Pisani *et al.*, Phys. Rev. B **75**, 064418 (2007).
- [12] O. Yazyev *et al.*, Phys. Rev. Lett. **100**, 047209 (2008).
- [13] J. Fernández-Rossier, Phys. Rev. B **77**, 075430 (2008).
- [14] H. Lee *et al.*, Phys. Rev. B **72**, 174431 (2005).
- [15] L. Malysheva and A. Onipko, arXiv:0802.1385v1.
- [16] K. Sasaki *et al.*, J. Phys. Soc. Jpn. **77**, 054703 (2008).
- [17] There are a number of reports of magnetism in damaged graphitic material which could be due to order along zigzag edge fragments. See, for example, H. Ohldag *et al.*, Phys. Rev. Lett. **98**, 187204 (2007).
- [18] M. Venkatesan *et al.*, Nature (London) **430**, 630 (2004).
- [19] M. I. Katsnelson, Mater. Today **10**, 20 (2007).
- [20] M. Y. Han *et al.*, Phys. Rev. Lett. **98**, 206805 (2007).
- [21] X. Li *et al.*, Science **319**, 1229 (2008).
- [22] S. S. Datta *et al.*, Nano Lett. **8**, 1912 (2008).